SOLAR WIND IONIC VARIATION ASSOCIATED WITH EARTHQUAKES GREATER THAN MAGNITUDE 6.0

Valentino STRASER
valentino.straser@alice.it

Gabriele CATALDI
ltpaobserverproject@gmail.com

ABSTRACT: The causes of earthquakes can be multiple and diverse, including those related with human activity. Various types of energy should then be evaluated besides the ones of tectonic origin, in order to build a specific modeling system of the data, which may support a probabilistic earthquake prediction in the short term. Among them, there are gravitational, inertial, electric and electromagnetic energies. The scientific question which the authors have tried to answer in the present study, is whether the global M6+ seismic activity is preceded by an increase in the solar activity, and in particular in the ionic variation of the solar wind. For this purpose, an analysis was performed on 428 earthquakes with greater than or equal to M6+ magnitude, which occurred on a global scale between 2012 and 2014. The data on seismicity have been compared with those provided by the geomagnetic observatories and those on the solar modulation transmitted by the ACE satellite orbiting the L1 point at 1.5 million kilometers from Earth. As the results reveal, the analyzed earthquakes with magnitude greater than M6+ have shown a remarkably higher occurrence during the phases of increase and decrease of the proton density of the solar wind.

Keywords*: Solar wind ionic variation, earthquake prediction, proton density*

INTRODUCTION

Background

The association between solar activity and strong earthquakes on a global scale has been hypothesized since the second half of the last Century and, on and off, resumed over the years by several authors (Simpson, 1967; Zhang, 1998; Han et al., 2004; Choi and Maslov, 2010). The electrically charged particles emitted from the Sun propagate through the heliosphere along the interplanetary magnetic field (IMF) reaching the planets of the solar system. When the solar wind reaches the Earth, it determines geomagnetic disruptions which interact with the Earth's magnetic field and with the ionosphere. The geomagnetic disruptions, which determine variations measurable with the use of electromagnetic sensors placed on the Earth's surface, have been associated with seismic events of high intensity (Mw ≥ 6) since the 1930's (Yanben et al., 2004).

In 1990, Takayama and Suzuki (1990) associated the Wolf number, i.e. the sunspot number, with destructive earthquakes occurred in Japan, while in 1967 Simpson suggested as a possible seismogenic mechanism the faradic current which is present in the Earth crust and produced by the solar activity. A few years later, in 2004, Han et al. found that large earthquakes were related to variations in the magnetic cycle of the solar activity. Mazzarella et al. (1988) concluded that the seismicity is related to solar activity and geomagnetic anomalies: they suggested that these two phenomena were capable of generating high intensity seismic events. A similar concept contemplating the effect of solar flares and magnetic storms was reasserted by Balasis et al. (2010). In 2011, Tavares and Azevedo suggested that an increase in solar activity coincides with an intensification of seismic events, while a study by the Space Environment Research Center of Kyushu University (Jusoh and Yumoto, 2011) revealed that 70% of great earthquakes (Mw 6-9) occurred within ±4 days, i.e. 4 days before or 4 days after, the arrival of the high-speed solar wind (HSSW). Variations in the solar electromagnetic radiation have been observed preceding great earthquakes, such as the one in Tohoku (He et al., 2012). A possible connection between solar and geomagnetic activity on a century-scale and an interaction mechanism between the two phenomena were proposed by Odintsov et al. (2006), while Straser and Cataldi (2014) recently suggested an interface mechanism of the solar and the geomagnetic activity as a triggering mechanism of strong earthquakes.

Geomagnetic activity and solar wind ionic variation

The variation in the Earth's geomagnetic activity is modulated by variations in ionic density, consisting of protons and electrons and present in the interplanetary medium that interacts with the Earth's

magnetosphere. The cause and effect relation between solar and geomagnetic activity affects the natural electromagnetic field in the SELF/ELF band. Such interference has been associated with potentially destructive earthquakes; variations were observed before five >M6.0 magnitude earthquakes in Mexico from 1999 to 2001 (Kotsarenko et al., 2004). Other variations of the geomagnetic field with frequency <3Hz were detected before earthquakes in: Armenia, Spitak (December 8, 1988, M=6.9); Loma Pietra, California, USA (October 18, 1989, M=7.1); Guam (August 8, 1993, M=8) (Hayakawa et al., 2007); and Izu Peninsula, Japan (July 1, 2000, M=6.4) (Ismaguilov et al., 2003). In 1964, a strong disturbance in the natural magnetic field with ≤10Hz frequency was recorded preceding the M9.2 earthquake that occurred in Kodiak, Alaska (Fraser-Smith, 2008). Radio emissions with <3Hz frequency were detected preceding the ML7.1 earthquake that occurred at Hotan of Xinjiang, China, October 19, 1996 (Du et al., 2004). Electromagnetic disturbance with frequency in the range of Pc3 geomagnetic pulsation (10-40s) were detected preceding the strong M6.4 earthquake that occurred on the island of Taiwan, China, December 19, 2009 (Takla et al., 2011). A study carried out from April 1997 to March 2002 by the RIKEN/UEC-NASDA scientific group reported electromagnetic anomalies in the SELF band preceding M6+ earthquakes (Hattori et al., 2004).

Strong radio emissions in the ELF band with 3-10 Hz frequency were detected preceding the strong MS8.0 earthquake that occurred in the Wenchuan County, China, May 12, 2008 (Li et al., 2013). Electromagnetic variations in the 0-15 Hz band preceded the M9.0 earthquake that occurred in Samoa, September 29, 2009 (Akhoondzadeh et al., 2013). Electromagnetic emissions in the 0-20 Hz band preceded the M7.0 earthquake that occurred in Haiti, January 12, 2010 (Athanasiou et al., 2011). Variations in the electromagnetic field between 0.25 and 0.5 Hz were detected preceding seismic events in Central Mexico from 2007 and 2009 (Chavez et al., 2010). Radio emissions in the SELF/ELF band were detected preceding the M5.5 earthquake that occurred in Bovec, Slovenia, July 12, 2004 (Prattes et al., 2008). In addition, strong variations in the geomagnetic field (included the presence of geomagnetic micropulsations) preceded the volcanic activity of Popocatepetl, Mexico, in the period March–July, 2005 (Kotsarenko et al., 2007). And radio emissions within 10.2 to 11.1 mHz and within 13.6 to 14.5 mHz frequency in the SELF band preceded the seismic activity in Central Mexico from 1999 to 2001 (Kotsarenko et al., 2005).

METHODS

The method adopted is deductive and based on an instrumental detection system. The data relating to the solar, seismic and geomagnetic activities, and to the radio emissions, were compared with each other to test any interconnection of electromagnetic type. The data on solar activity and seismic activity were real-time retrieved from the websites.

DATA

The data on the solar activity concern the variation in the ionic density of the solar wind detected by the ACE (Advanced Composition Explorer) satellite orbiting the L1 point (Lagrange point) at 1.5 million kilometers from Earth; Solar Wind Density (ENLIL Heliosphere Ecliptic Plane), variations in interplanetary magnetic field or IMF (GOES); X-ray flux (GOES), temporal monitoring of CMEs events or Solar Coronal Mass Ejections (ISWA); monitoring of the coronal holes position on the Sun's surface (NSO/SOLIS-VSM Coronal Hole); Solar Wind Velocity (ENLIL Helisphere Ecliptic Plane); Electron flux (NOAA/SWPC); Magnetopause Standoff Distance (CCMC/RT).

The data on geomagnetic activity were retrieved from: AL-Index (WINDMI and Kyoto WDC); DST-Index (WINDMI and Kyoto WDC); Driving Input Voltage VSW (WINDMI); Hemispheric Power (NOAA/POES); Total Electron Content (TEC SWACI map); Electron Density (Electron Density map JRO); variations in the geomagnetic field (provided by geomagnetic observatories: Tromso, Sodankyla, Kiruna, Licksele, Cobenzel, USGS, INGV, Canberra, Scoresbysund, Denmark, Narsarsuaq, Kullorsuaq); Estimated Kp-Index (NOAA/SWPC) A-Index (Tromso Geomagnetic Observatory); variations in polar electromagnetic emission (GOES/METP). The data relating to the pre-seismic radio emissions were provided by the SELF/ELF induction magnetometer of the Radio emissions Project (Lat: 41°41'4 .27"N, Long: 12°38'33,60"E, Albano Laziale, Rome, Italy), which reads the intensity and frequency of the Earth's magnetic field every 60 seconds on the Z magnetic component.

The data on the global seismic activity on the M6+ scale were real-time retrieved from USGS (United States Geological Survey), CSEM or EMSC (Centre Sismologique Euro-Méditerranéen or European-Mediterranean Seismological Centre) and GFZ (Deutsches GeoForchungs Zentrum or German Research Centre for Geosciences), and used within 48 hours from publication.

RESULTS

The analysis of the ionic variation of the solar wind in the interplanetary medium has allowed to determine that the earthquakes had occurred after a gradual variation, i.e. lasting more than 24 hours, in the proton density with energy subdivided into five groups: 1060-1900 keV, 795-1193 keV, 310-580 keV, 115-195 keV, 47-68 keV.

The flux of ions from the Sun that reaches the Earth is mainly due to explosions that occur in the solar flare. Fluxes of ions are also originated from coronal holes (50) and are high-density fluxes.
In some cases, the increase of the electron density was superimposed on the increase of the proton density, with energy distributed into two groups: 175-315 keV e 38-53 keV (**Fig. 1**). The final point of the first wave and the starting point of the following one has been defined as "Start Point", i.e. the starting point of what is considered a candidate to interplanetary seismic precursor. It corresponds to the relative basic level that separates the proton increments.

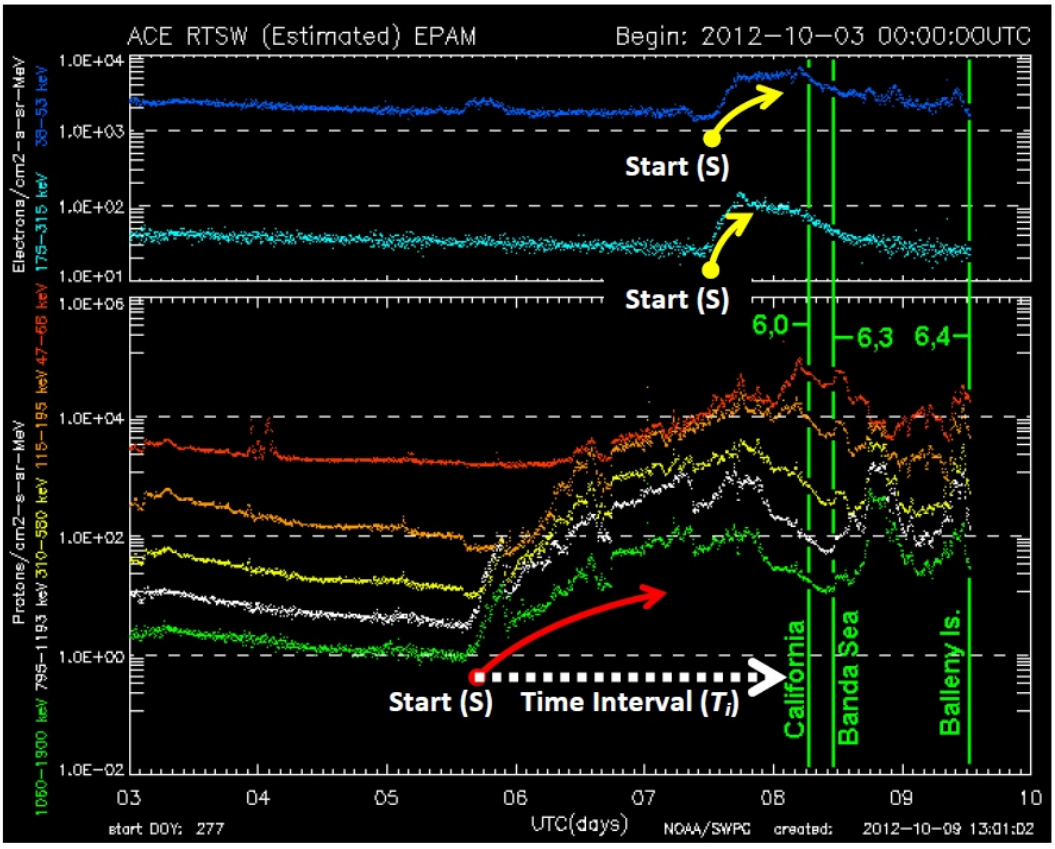

Figure 1. Densitogram of the ions in the interplanetary medium at L1 Lagrange point. Data recorded by ACE (Advanced Composition Explorer) Satellite, October 3-9, 2012. The vertical green lines indicate the time markers for M6+ earthquakes occurred on a global scale, October 8-9, 2012; the green numbers indicate the magnitude (Mw). The red arrow indicates the start (S) and direction of the "gradual" proton increase recorded preceding the M6+ earthquakes. The two yellow arrows indicate the start of the "gradual" electronic increase that preceded the earthquakes examined. The horizontal white arrow indicates the time interval (T*i*) which separates the start of the increase in the proton density and the associated seismic event.

A problem arises when measuring the basic level between two proton increments because of one increment superimposing on the other. The phenomenon, which happens frequently, of a proton increment being superimposed on another one is due to the Sun's dynamics and therefore to the various causes that can produce an ion ejection. When two proton increments overlap leading to the formation of a longer wave, the two waves are simply added together, and the observation of the decrease of ionic density in the following days will identify the basic level.

Referring to **Fig. 2**, which outlines the curve of the proton density variation observed preceding potentially destructive earthquakes in the years 2012, 2013 and 2014, four time intervals were analyzed as follows:
A) during the increase phase of the proton density;
B) at the maximum value recorded of the proton density;
C) during the decrease phase of the proton density;
D) after the complete decrease of the proton density which restored to the basic level.

Basic level in this study refers to the proton density whose energy is included within 1220 and 761 keV (values derived from the ISWA charts) and within 1900 and 1060 keV (EPAM charts). The basic level of protons that have this type of energy corresponds exactly to 0.1-0.5 particles / cm^2/s.

From the experimental observations on M6+ earthquakes occurred in the period between 2012 and 2014 as listed in **Table 1**, the frequencies resulted as follows in the Discussion section.

Tab. 1 Number of M6+ earthquakes that occurred on a global scale in the years 2012, 2013, 2014, compared with the total 428 of the three years considered, in the intervals A, B, C, D (Fig. 2).

	2012	**2013**	**2014**
Interval A 145/428 (33,96%)	42/133	46/142	57/153
Interval B 32/428 (7,49%)	14/133	11/142	7/153
Interval C 214/428 (50,12%)	70/133	70/142	74/153
Interval D 36/428 (8,43%)	7/133	15/142	14/153
Number of M6+ earthquakes	133	142	153

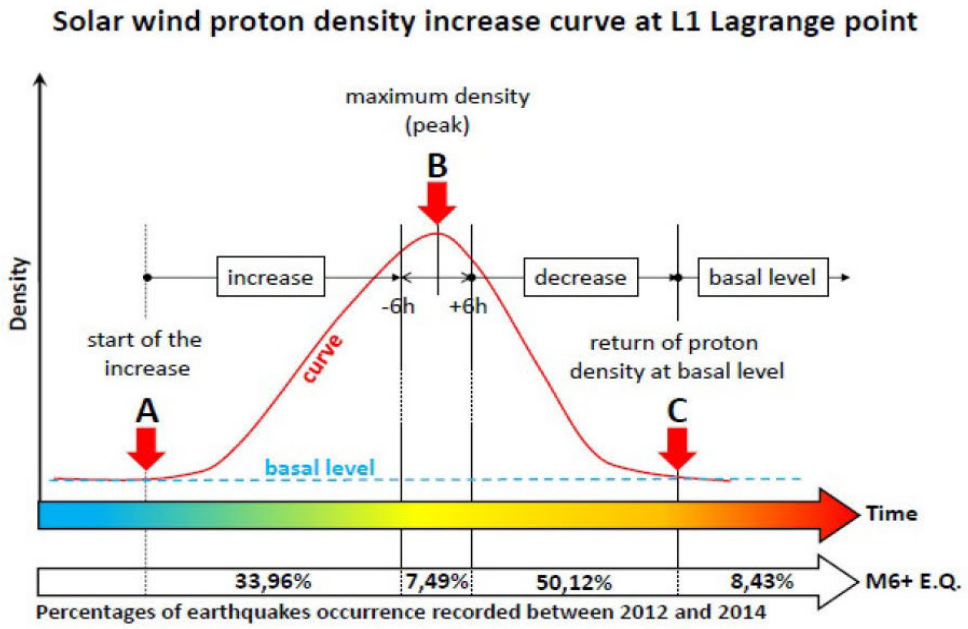

Figure 2. Increase in the proton density of the solar wind as represented in Figure 1, which precedes the earthquakes examined. A refers to the increase phase of the proton density; B refers to the maximum value recorded of the proton density (±6 from the max.); C refers to the decrease phase of the proton density; D refers to the complete decrease of the proton density which restored to the basic level. Where A+B+C+D= 428/428 earthquakes (100%).

DISCUSSION

Between 2012 and 2014, the global seismicity began to increase (**Table 1)** while the solar activity was subject to fluctuations, as reported in the NOAA data (http://services.swpc.noaa.gov/images/solar-cycle-planetary-a-index.gif), after its rise culminated in 2012. In the time interval considered, the solar activity began to weaken and fluctuate because of the absence of spot groups, gathered in extended solar regions.

As illustrated in **Figure 3**, the distribution of earthquakes along the curve of the proton density variation is repeated every year approximately at the same percentage, regardless of the number of M6+ earthquakes. This indicates that the observed phenomenon is objective and recurring.

Table 2. M6+ earthquakes frequency (%) in the intervals A, B, C, D (Fig. 2) in the years 2012, 2013, 2014.

	2012	2013	2014	Average 2012-2014
P_A	31.58%	32.39%	37.50%	33.88%
P_B	10.53%	7.75%	4.61%	7.48%
P_C	52.63%	49.30%	48.68%	5.23%
P_D	5.26%	10.56%	9.21%	8.41%

Assuming that the M6+ seismic events were completely unrelated to the occurrence of solar events, the probability that a seismic event occurred in a definite phase would be equal to the average relative duration of that phase. Considering that the average duration of the complete cycle is T_{Tot}=11.21 days (100%), each phase has a duration: T_A=1.01 days, T_B=1.68 days, T_C=3.1 days, T_D=5.42 days, it follows that:

$$P_{unrelated\ A} = T_A / T_{Tot} = 9\%$$
$$P_{unrelated\ B} = T_B / T_{Tot} = 14.89\%$$
$$P_{unrelated\ C} = T_C / T_{Tot} = 27.65\%$$
$$P_{unrelated\ D} = T_D / T_{Tot} = 48.34\%$$

Thus, the values are consistent within the three years analyzed and considerably different from those deriving from the hypothesis that the two phenomena are unrelated.

The following calculation does not compare $P_{unrelated}$ with single years but with an average value over the complete period, since the durations of A, B, C and D, wherefrom $P_{unrelated\ A}$, $P_{unrelated\ B}$, $P_{unrelated\ C}$, $P_{unrelated\ D}$ derive, are average durations over the whole period and not per single year; comparing homogeneous data seems therefore legitimate.

The odds ratio of occurrence may be understood more correctly as the ratio of observed frequency and expected frequency on the assumption of independent phenomena. Rather than the data reliability, this value denotes more appropriately what indications emerge from the data, and whether they are solid and consistent. When the values are all close to 1, there is no link between the two phenomena, whereas if some of the values are remarkably far from 1, a link is assumed to be present.

The data cannot be evaluated singularly but as a whole since it is obvious that if one is greater than 1, the other data will be less than 1 due to a compensation effect. In particular, determining the odd ratio between two occurrence probabilities, it follows that:

$$P_{A\ mean} / P_{unrelated\ A} = 3.76$$
$$P_{B\ mean} / P_{unrelated\ B} = 0.49$$
$$P_{C\ mean} / P_{unrelated\ C} = 1.81$$
$$P_{D\ mean} / P_{unrelated\ D} = 0.17$$

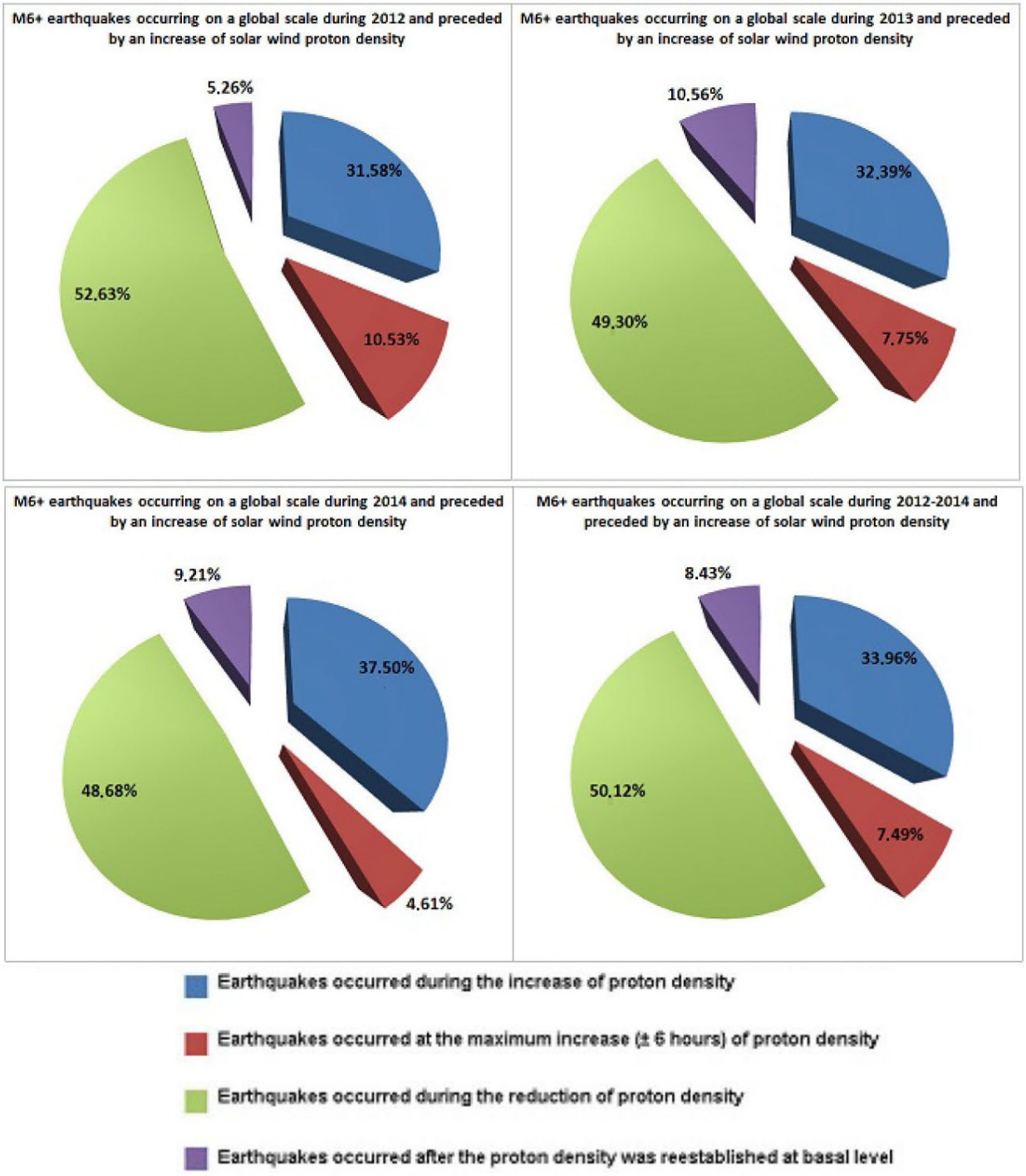

Figure 3. M6+ earthquakes occurring on a global scale during 2012-2014 and preceded by an increase of solar wind proton density in the intervals A+B+C+D represented in Fig. 2.

Observing the data, it results that there is a much greater frequency of M6+ seismic events in the (A) increase and (C) decrease phases compared with the hypothesis of unrelated phenomena, whereas in the peak phase (B) and the basic level (D) the detected frequency is much lower.

Rather than establishing a connection with the intensity of the solar phenomenon, this behavior suggests a link with the variation in its intensity and the global seismic activity with magnitude greater than >M6 on the Richter Scale. If an ionic variation is in progress, earthquakes occur more frequently, while if the proton density levels off avoiding any further increase or decrease, the earthquakes occur less frequently. Thus, the disturbances in the geomagnetic field happen irrespective of its absolute value, i.e. the maximum or minimum value reached at a given time, but only considering the oscillations that occur over a time period.

However, if we consider the data aiming at short-term prediction, we see that the average time interval (T*i*) recorded between the start (S) of the "gradual" increase in the proton density and the M6+ earthquakes occurred on a global scale, was 146 hours. The maximum time interval, 784 hours, was recorded preceding the M7.0 earthquake that occurred in Indonesia, April 6, 2013. The minimum time interval, 1 hour, was recorded during the M6.0 earthquake that occurred in Mariana Islands, November 19, 2013, the M6.5 earthquake in Barbados, February 18, 2014 and the M6.0 earthquake in Papua New Guinea, M6.0, May 10, 2014.

CONCLUSION

The analysis of the data shows a connection between the earthquakes examined in this study and the gradual increase of ionic density of the interplanetary medium (**Fig. 1**) caused by a solar flare or by the presence of a coronal hole. Since the ionic increase of the interplanetary medium is derived from an increase in the solar activity and since the M6+ earthquakes occurred on a global scale in the time period from 2012 and 2014 were preceded by an ionic increase in the solar wind, this approach could be tested to promptly predict a resumption of M6+ seismic activity on a global scale.

In conclusion, we believe that it would be worth investigating in further studies and projects, and in an interdisciplinary context, the possible link between the ionic increase of the interplanetary medium with potentially destructive earthquakes of magnitude greater than or equal to M6.

ACKNOWLEDGMENTS: The authors thank the physicist Dr Alessandro Ferrari for his critical reading of the manuscript, Dr Daniele Cataldi for the scientific support, and Dr Sara Ghirardi for the linguistic revision.

REFERENCES CITED

Akhoondzadeh, M., 2013. Novelty detection in time series of ULF magnetic and electric components obtained from DEMETER satellite experiments above Samoa (29 September 2009) earthquake region. *NHSS (Natural Hazards and Earth System Sciences)*, v. 13, p. 15–25.

Abdussamatov, H.I., 2012. Bicentennial Decrease of the Total Solar Irradiance Leads to Unbalanced Thermal Budget of the Earth and the Little Ice Age. *Applied Physics Research*, v. 4, no. 1; February 178 ISSN 1916–9639 E-ISSN 1916–9647.

Athanasiou, M.A., Anagnostopoulos, G.C., Iliopoulos, A.C., Pavlos, G. P. and David, C.N., 2011. Enhanced ULF radiation observed by DEMETER two months around the strong 2010 Haiti earthquake. *NHSS (Natural Hazards and Earth System Sciences)*, v. 11, p. 1091–1098.

Balasis, G., Daglis, I.A., Anastasiadis, A., Papadimitriou, C., Mandea, M. and Eftaxias, K., 2011. Universality in solar flare, magnetic storm and earthquake dynamics using Tsallis statistical mechanics. *Physica A*, no. 390, p. 341–346.

Chavez, O., Millan-Almaraz, J.R., Perez-Enriquez, R., Arzate-Flores, J.A., Kotsarenko, A., Cruz-Abeyro, J.A. and Rojas, E., 2010. Detection of ULF geomagnetic signals associated with seismic events in Central Mexico using Discrete Wavelet Transform. *NHSS (Natural Hazards and Earth System Sciences)*, v. 10, p. 2557–2564.

Choi, D. R. and Maslov, L., 2010. Earthquakes and solar activity cycles. *New Concepts in Global Tectonics Newsletter*, no. 57, p. 85–97.

Du, A., Zhou, Z., Xu W. and Yang, S. 2004. Generation Mechanism of ULF electromagnetic emissions before the ML = 7.1 earthquake at Hotan. *Chinese Journal of Geophysics*, v. 47, no. 5, p. 939–945.

Fraser-Smith, A. C., 2008., Ultralow-Frequency Magnetic Fields Preceding Large Earthquakes, Departments of Electrical Engineering and Geophysics, Stanford University, Stanford, Calif. *FORUM, EOS*, v. 89, no. 23, p. 211.

Hattori, K., Takahashi, I., Yoshino, C., Isezaki, N., Iwasaki, H., Harada, M., Kawabata, K., Kopytenko, E., Kopytenko, Y., Maltsev, P., Korepanov, V., Molchanov, O., Hayakawa, M., Noda, Y., Nagao, T. and Uyeda, S., 2004. ULF geomagnetic field measurements in Japan and some recent results associated with Iwateken Nairiku Hokubu Earthquake in 1998. *Phys. Chem. Earth*, v. 29, p. 481–494.

Hayakawa, M., Hattori, K. and Ohta, K., 2007. Monitoring of ULF (ultra-low-frequency) Geomagnetic Variations Associated with Earthquakes. *Sensor*, v. *7*, n.o 7, p. 1108–1122.

He, L., Wu, L., Pulinets, S., Liu, S. and Yang. F., 2012. A nonlinear background removal method for seismo-ionospheric anomaly analysis under a complex solar activity scenario: A case study of the M9.0 Tohoku

earthquake. *Advances in Space Research*, v. 50, p. 211–220.

Jusoh, M.H. and Yumoto, K., 2011. Possible correlation between solar activity and global seismicity. Space Environment Research Center of Kyushu University, ISW/MAGDAS School, Lagos, Nigeria. Proceedings.

Kotsarenko, A., Perez Enriquez, R., Lopez Cruz-Abeyro, J.A., Koshevaya, S., Grimalsky, V. and Zuniga, F.R., 2004. Analysis of the ULF electromagnetic emission related to seismic activity, Teoloyucan geomagnetic station, 1998–2001. *NHSS (Natural Hazards and Earth System Sciences)*, v. 4, p. 679–684, SRef-ID: 1684–9981/nhess/2004-4-679, European Geosciences Union.

Kotsarenko, A., Molchanov, O., Perez Enriquez, R., Lopez Cruz-Abeyro, J. A., Koshevaya, S., Grimalsky, V. and Kremenetsky, I., 2005.Possible seismogenic origin of changes in the ULF EM resonant structure observed at Teoloyucan geomagnetic station, Mexico, 1999–2001. *NHSS (Natural Hazards and Earth System Sciences)*, v. 5, p. 711–715.

Kotsarenko, A., Grimalsky, V., Perez Enriquez, R., Valdez-Gonzalez, C., Oshevaya, S., Lopez Cruz-Abeyro, J. A. and Yutsis , V., 2007. Volcano Popocatepetl, Mexico: ULF geomagnetic anomalies observed at Tlamacas station during March-July, 2005. *NHSS (Natural Hazards and Earth System Sciences)*, v. 7, p. 103–107.

Ismaguilov, V.S., Kopytenko, Yu.A., Hattori, K. and Hayakawa, M., *2003.* Variations of phase velocity and gradient values of ULF geomagnetic disturbances connected with the Izu strong earthquakes. European Geosciences Union 2003, *NHSS (Natural Hazards and Earth System Sciences)*, v. 3, p. 211–215.

Li, M., Lu, J., Parrot, M., Tan, H., Chang, Y., Zhang, X. and Wang, Y., 2013. Review of unprecedented ULF electromagnetic anomalous emissions possibly related to the Wenchian Ms = 8,0 earthquake, on 12 May 2008, *NHSS (Natural Hazards and Earth System Sciences)*, v. 13, p. 279–286.

Mazzarella, A. and Palumbo, A., 1988. Solar, geomagnetic and seismic activity. *Nuovo Cimento C*, Serie 1, v. 11c, p. 353–364.

Odintsov, S., Boyarchuk, K., Georgieva, K., Kirov, B. and Atanasov, D., 2006. Long-period trends in global seismic and geomagnetic activity and their relation to solar activity. *Physics and Chemistry of the Earth*, v. 31, p. 88–93.

Prattes, G., Schwingenschh, K., Eichelberger H.U., Magnes, W.M., Boudjada, M., Stachel, M., Vellante, M., Wesztergom, V. and Nenovski, P., 2008. Multi-point ground-based ULF magnetic field observations in Europe during seismic active periods in 2004 and 2005. *NHSS (Natural Hazards and Earth System Sciences)*, v. 8, p. 501–507.

Simpson, J.F., 1967. Solar activity as a triggering mechanism for earthquakes. *Earth and Planetary Science Letters*, v. 3, p. 417–425.

Straser, V. and Cataldi, G., 2014. Solar wind proton density increase and geomagnetic background anomalies before strong m6+ earthquakes, p. 280-286. Proceedings of MSS–14, Space Research Institute, Moscow.

Takayama, T. and Suzuki, T., 1990. On the relation between the sunspot number and the destructive earthquakes in Japan. *Bull. Earthquake Research Institute of Tokyo Imperial University*, v. 8, no. 3, p. 373–374.

Takla, E. M., Yumoto, K., Liu, J. Y., Kakinami, Y., Uozumi, T., Abe, S. and Ikeda, A., 2011. Anomalous geomagnetic variations possibly linked with the Taiwan earthquake (Mw = 6.4) on 19 December 2009. *International Journal of Geophysics*, vol. 2001, Article ID 848467, p. 10.

Tavares, M. and Azevedo, A., 2011. Influences of solar cycles on earthquakes. *Natural Science 3*, v. 3, no. 6, p. 436–443.

Yanben, H., Zengjian, G., Jibing, W. and Lihua, M., 2004. Possible triggering of solar activity to big earthquakes (Ms ≥ 8) in faults with near west-east strike in China. *Science in China Ser. G. Physics, Mechanics and Astronomy*. v. 47, no. 2, p. 173–181.

Zhang, G-Q., 1998. Relationship between global seismicity and solar activities. A*cta Seismologica Sinica*, v. 11, p. 495–500.

Websites cited

E.M.S.C. – European-Mediterranean Seismological Centre – http://www.emsc-csem.org/

Harvard-Smithsonian Center for Astrophysics – https://www.cfa.harvard.edu/

I.N.G.V. – Istituto Nazionale di Geofisica e Vulcanologia – http://cnt.rm.ingv.it/

I.S.W.A. – Integrated Space Weather Analysis System – http://iswa.ccmc.gsfc.nasa.gov/IswaSystemWebApp /

N.A.S.A. – National Aeronautics and Space Administration – http://www.nasa.gov/

N.O.A.A. – National Oceanic and Atmospheric Administration – http:// www.noaa.gov/

S.A.O./N.A.S.A. Astrophysics Data System – http://adswww.harvard.edu/

U.S.G.S. – United States Geological Survey – http://earthquake.usgs.gov/

APPENDIX

Study of relationship between solar wind proton density variation and M6+ global seismic activity.

Total: 428 earthquakes, of which:

133 occurred in 2012

142 occurred in 2013

153 occurred in 2014

***Time lag recorded between the **ISP Start** and the **earthquake**

A: during the phase of increasing.

B: at the maximum level of proton density recorded (± 6 hours from the maximum).

C: during the phase of reduction of the proton density.

D: after complete reduction of proton density that has been reestablished to baseline.

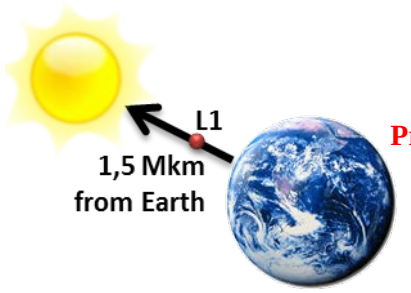

Protonic density on interplanetary medium at Lagrange point L1

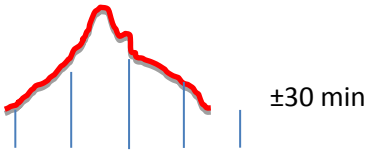

Location Earthquake	Magnitude Mw	Data M/D/Y	HH:MM (UTC)	A	B	C	D		*Time Lag (hours)
Izu Idlands	6.2	Jan. 01,2012	05:27			X			183
Santa Cruz Islands	6.4	Jan. 09,2012	04:07				X		374
Northern Sumatra	7.2	Jan. 10,2012	18:36				X		384
South Shetland Islands	6	Jan. 15,2012	13:40	X					43
South Shetland Islands	6	Jan. 15,2012	14:41	X					44
Offshore Chiapas, Mexico	6.2	Jan. 20,2012	18:47	X					168
Sandwich Islands Region	6	Jan. 22,2012	05:53		X				203
Offshore Bio-Bio Chile	6.1	Jan. 23,2012	16:04	X					238
Fiji Islands	6.3	Jan. 24,2012	00:52	X					254
Near the coast of central Peru	6.4	Jan. 30,2012	05:11			X			403
Vanuatu	7.1	Feb. 02,2012	13:34			X			483
Vanuatu	6.1	Feb. 03,2012	03:46			X			497
Vanuatu	6.1	Feb. 05,2012	00:15			X			541
Vanuatu	6.1	Feb. 05,2012	16:40			X			557
Negros	6.7	Feb. 06,2012	03:49			X			568
Negros	6	Feb. 06,2012	10:10			X			574
Solomon Islands	6.4	Feb. 14,2012	08:19		X				75
Fiji Islands	6	Feb. 26,2012	05:21	X					91
Siberia, Russia	6.7	Feb. 26,2012	06:17	X					90
Loyalty Islands	6.6	Mar.03,2012	12:19			X			242
Santiago Del Estero	6.1	Mar.05,2012	07:46	X					25
Vanuatu	6.7	Mar.09,2012	07:09			X			121
Honshu, Japan	6.9	Mar.14,2012	09:08			X			243
Honshu, Japan	6.1	Mar.14,2012	10:49			X			244
Honshu, Japan	6	Mar.14,2012	12:05			X			246
Papua New Guinea	6.2	Mar.14,2012	21:13			X			255
Papua, Indonesia	6.1	Mar.20,2012	17:56			X			275
Oaxaca, Mexico	7.4	Mar.20,2012	18:02			X			276
Papua New Guinea	6.6	Mar.21,2012	22:15			X			300
Maule, Chile	7.1	Mar.25,2012	22:37	X					51
East Pacific Rise	6	Mar.26,2012	18:12	X					71
Honshu, Japan	6.1	Mar.27,2012	11:00	X					88
Oaxaca, Mexico	6	Apr.02,2012	17:36			X			238
Papua New Guinea	6.1	Apr.06,2012	16:15	X					42
Northern Sumatra	8.6	Apr.11,2012	08:38		X				53
North Indian Ocean	6	Apr.11,2012	09:27		X				54
Northern Sumatra	8.2	Apr.11,2012	10:43		X				55
Coast of Oregon	6	Apr.11,2012	22:41			X			57

Michiacan, Mexico	6.5	Apr.11,2012	22:55			X			57
Baja California, Mexico	6.5	Apr.12,2012	07:06			X			66
Baja California, Mexico	7	Apr.12,2012	07:15			X			66
Drake Passage	6.2	Apr.14,2012	10:56			X			117
Vanuatu	6.2	Apr.14,2012	22:05				X		129
Northern Sumatra	6.2	Apr.15,2012	05:57				X		136
Valparaiso, Chile	6.7	Apr.17,2012	03:50	X					16
Papua New Guinea	6.8	Apr.17,2012	07:13	X					19
Sandwich Islands	6.2	Apr.17,2012	19:03	X					32
Papua, Indonesia	6.7	Apr.21,2012	01:16	X					110
Papua, Indonesia	6	Apr.21,2012	01:25	X					110
Kermadec Islands	6	Apr.23,2012	17:36			X			174
Tonga	6.6	Apr.28,2012	10:08				X		49
Chiapas, Mexico	6	May 01,2012	22:43			X			55
Tarapaca	6.2	May 14,2012	10:00	X					73
Coast of Aisen, Chile	6.3	May 18,2012	02:00		X				27
Northern Italy	6	May 18,2012	02:03		X				27
Honshu, Japan	6.3	May 18,2012	07:20		X				32
Indian-Antarctic Ridge	6	May 23,2012	22:59			X			167
Norvegian Sea	6.1	May 24,2012	22:47			X			191
Bonin Islands	6	May 26,2012	21:48	X					27
Santiago Del Estero	6.7	May 28,2012	05:07		X				58
South of Panama	6.3	June 03,2012	00:45			X			31
South of Panama	6.3	June 04,2012	03:15			X			60
Honshu, Japan	6.1	June 05,2012	19:31			X			97
Maule, Chile	6	June 07,2012	04:05			X			130
Southern Peru	6.1	June 08,2012	16:03			X			142
Dodecanese Islands, Greece	6.3	June 12,2012	12:44	X					258
Honshu, Japan	6.3	June 17,2012	20:32			X			74
Aleutian Islands, Alaska	6	June 19,2012	15:56			X			117
Northern Sumatra	6.1	June 23,2012	04:34			X			202
Kamchatka Peninsula, Russia	6	June 24,2012	03:15			X			225
Northern Xinjiang, China	6.3	June 29,2012	21:07	X					26
Cook Strait, New Zealand	6.3	July 03,2012	10:36			X			111
Vanuatu	6.3	July 06,2012	02:28	X					27
Kuril Islands	6	July 08,2012	11:32	X					84
Kuril Islands	6	July 20,2012	06:10			X			189
Simeulue, Indonesia	6.4	July 25,2012	00:27			X			303
Solomon Islands	6.4	July 25,2012	11:20			X			314
Mauritius, Reunion Region	6.7	July 26,2012	05:33			X			332
Papua New Guinea	6,5	July 28,2012	20:03			X			395
Central Perù	6.1	Aug. 02,2012	09:38	X					106
Papua New Guinea	6.1	Aug. 02,2012	09:56	X					106
Fox Islands, Alaska	6.2	Aug. 10,2012	18:37			X			139
Northwestern Iran	6.4	Aug. 11,2012	12:23			X			157
Northwestern Iran	6.2	Aug. 11,2012	12:34			X			157
Xinjiang-Xizang border region	6.2	Aug. 12,2012	10:37			X			179
Sea of Okhotsk	7.7	Aug. 14,2012	02:59			X			219
Sulawesi, Indonesia	6.3	Aug. 18,2012	09:41	X					13
Papua New Guinea	6.2	Aug. 19,2012	22:41	X					50
Molucca sea	6.6	Aug. 26,2012	15:05			X			211
El Salvador	7.3	Aug. 27,2012	04:37			X			224
Jan Mayen Island	6.8	Aug. 30,2012	13:43			X			305
Philippine Islands region	7.6	Aug. 31,2012	12:47			X			329
Java, Indonesia	6.1	Sept. 03,2012	18:23		X				62
Santa Cruz Islands	6	Sept. 05,2012	13:09			X			107
Costa Rica	7.6	Sept. 05,2012	14:42			X			108
Papua, Indonesia	6.1	Sept. 08,2012	10:51			X			177
Kepulauan Mentawai region	6.2	Sept. 13,2012	23:59			X			309
Baja California, Mexico	6.3	Sept. 25,2012	23:45	X					94
Aleutian Islands, Alaska	6.4	Sept. 26,2012	23:59	X					109
Colombia	7.3	Sept. 30,2012	16:31		X				207
Honshu, Japan	6.1	Oct. 01,2012	22:31			X			237
Banda Sea	6.1	Oct. 08,2012	11:43			X			69
Macquarie Island	6.6	Oct. 09,2012	12:32			X			95
Papua, Indonesia	6.6	Oct. 12,2012	00:31			X			155
Celebes Sea	6	Oct. 17,2012	04:42	X					8
Vanuatu	6.2	Oct. 20,2012	23:00			X			99
Costa Rica	6.5	Oct. 24,2012	00:45			X			173
Canada	7.8	Oct. 28,2012	03:04	X					9
Canada	6.3	Oct. 28,2012	18:54	X					25
Canada	6.2	Oct. 30,2012	02:49	X					56

Mindanao	6.1	Nov. 02,2012	18:17				X		144
Guatemala	7.4	Nov. 07,2012	16:36	X					88
Vancouver Island	6.1	Nov. 08,2012	02:01	X					98
Central Perù	6	Nov. 10,2012	14:57	X					53
Myanmar	6.8	Nov. 11,2012	01:12	X					64
Guatemala	6,5	Nov. 11,2012	22:14	X					85
Gulf of Alaska	6.3	Nov. 12,2012	20:42		X				107
Aisen, Chile	6.1	Nov. 13,2012	04:31		X				115
Coquimbo, Chile	6.1	Nov. 14,2012	19:02			X			154
Guerrero, Mexico	6.1	Nov. 15,2012	09:20			X			168
Kuril Islands	6.5	Nov. 16,2012	18:12			X			199
Papua New Guinea	6	Nov. 19,2012	09:44			X			30
Vanuatu	6.1	Dec. 02,2012	00:54			X			310
Honshu, Japan	7.3	Dec. 07,2012	08:18	X					27
Honshu, Japan	6.2	Dec. 07,2012	08:31	X					27
North Island of New Zealand	6.3	Dec. 07,2012	18:19	X					37
Banda Sea	7.1	Dec. 10,2012	16:53			X			107
Molucca sea	6.6	Dec. 11,2012	06:18			X			145
California	6.3	Dec. 14,2012	10:36	X					18
Aleutian Islands, Alaska	6	Dec. 15,2012	04:49		X				36
Papua New Guinea	6.1	Dec. 15,2012	19:30			X			51
Sulawesi, Indonesia	6.1	Dec. 17,2012	09:16			X			91
Vanuatu	6.7	Dec. 21,2012	22:28				X		198
									133 Earthquakes
Alaska	7.5	Jan. 05,2013	08:58				X		180
Pacific-Antarctic Ridge	6.1	Jan. 15,2013	16:09	X					76
Indonesia	6.1	Jan. 21,2013	22:22			X			121
Kazakhstan	6.1	Jan. 28,2013	16:38			X			57
Chile	6.8	Jan. 30,2013	20:15			X			108
Solomon Islands	6.1	Jan. 30,2013	23:03			X			111
Solomon Islands	6.1	Jan. 31,2013	03:33			X			115
Solomon Islands	6	Feb. 01,2013	05:36	X					3
Solomon Islands	6.4	Feb. 01,2013	18:33	X					15
Solomon Islands	6.3	Feb. 01,2013	22:16	X					19
Japan	6.9	Feb. 02,2013	14:17	X					35
Solomon Islands	6	Feb. 02,2013	18:58	X					39
Solomon Islands	6	Feb. 06,2013	00:07			X			117
Solomon Islands	8	Feb. 06,2013	01:12			X			118
Solomon Islands	7.1	Feb. 06,2013	01:23			X			118
Solomon Islands	7	Feb. 06,2013	01:54			X			119
Solomon Islands	6	Feb. 06,2013	10:33			X			127
Solomon Islands	6	Feb. 06,2013	11:53			X			129
Solomon Islands	6	Feb. 07,2013	00:30			X			141
Solomon Islands	6.7	Feb. 07,2013	18:59	X					159
Solomon Islands	6.8	Feb. 08,2013	11:12		X				15
Solomon Islands	7.1	Feb. 08,2013	15:26		X				19
Colombia	6.9	Feb. 09,2013	14:16			X			42
Solomon Islands	6.6	Feb. 09,2013	21:02			X			49
Solomon Islands	6	Feb. 09,2013	18:39			X			166
Russia	6.6	Feb. 14,2013	13:13	X					28
Philippines	6.1	Feb. 16,2013	04:37			X			67
Argentina	6.1	Feb. 22,2013	12:01			X			219
Russia	6.9	Feb. 28,2013	14:05			X			110
Russia	6.4	Mar. 01,2013	12:53			X			133
Russia	6.5	Mar. 01,2013	13:20			X			133
Papua New Guinea	6.5	Mar. 10,2013	22:51	X					154
Fiji	6.1	Mar. 24,2013	08:13			X			476
Guatemala	6.2	Mar. 25,2013	23:02			X			515
Japan	6	Apr. 01,2013	18:53		X				678
Russia	6.3	Apr. 05,2013	13:00				X		769
Indoneia	7	Apr. 06,2013	04:42				X		784
Iran	6.4	Apr. 09,2013	11:52	X					28
Vanuatu	6	Apr. 13,2013	22:49		X				104
Papua New Guinea	6.6	Apr. 14,2013	01:32		X				138
Iran	7.7	Apr. 16,2013	10:44			X			195
Papua New Guinea	6.6	Apr. 17,2013	23:55			X			232
Russia	7.2	Apr. 19,2013	03:05	X					9
Russia	6.1	Apr. 19,2013	19:58	X					25
China	6.6	Apr. 20,2013	00:02	X					30
Russia	6.1	Apr. 20,2013	13:12	X					43
Izu Islands, Japan	6.1	Apr. 21,2013	03:22	X					57
Papua New Guinea	6.5	Apr. 23,2013	23:14			X			125

New Zealand	6.1	Apr. 26,2013	06:53		X				25
New Zealand	6.2	Apr. 26,2013	06:53		X				25
Solomon Islands	6	May 06,2013	10:33			X			127
Ceva-i-Ra, Fiji	6	May 07,2013	10:10			X			118
Iran	6.1	May 11,2013	02:08	X					40
Tonga	6.4	May 11,2013	20:46	X					58
Mariana Islands	6.8	May 14,2013	00:32	X					110
Japan	6	May 18,2013	05:47		X				211
Chile	6.4	May 20,2013	09:49			X			264
Russia	6	May 21,2013	01:55			X			279
Russia	6.1	May 21,2013	05:43			X			253
Tonga	7.4	May 23,2013	17:19	X					28
Tonga	6.3	May 23,2013	21:07	X					32
Sea of Okhotsk	8.3	May 24,2013	05:44	X					40
Sea of Okhtsk	6.7	May 24,2013	14:46	X					49
Taiwan	6.2	June 02,2013	05:43		X				67
Solomon Islands	6,1	June 05,2013	04:47			X			138
Christmas Island	6.7	June 13,2013	16:47				X		342
Kermadec Islands	6	June 15,2013	11:20				X		385
Greece	6.2	June 15,2013	16:11				X		390
Nicaragua	6.5	June 15,2013	17:34				X		391
Greece	6	June 16,2013	21:39				X		10
Northern Mid-Stlantic Ridge	6.6	June 24,2013	22:04			X			202
Indonesia	6.1	July 02,2013	07:37			X			98
Papua New Guinea	6.1	July 04,2013	17:16			X			156
Indonesia	6	July 06,2013	05:05	X					18
Papua New Guinea	7.3	July 07,2013	18:35	X					55
Papua New Guinea	6.6	July 07,2013	20:30	X					57
Sandwich Islands	7.3	July 15,2013	14:03	X					50
Papua New Guinea	6	July 16,2013	09:35	X					69
Peru	6	July 17,2013	02:37	X					86
New Zealand	6.5	July 21,2013	05:09			X			185
Prince Edward Islands	6.1	July 22,2013	07:01			X			211
Vanuatu	6.1	July 26,2013	07:07			X			307
Sandwich Islands	6,2	July 26,2013	21:32			X			321
Tonga	6	Aug. 01,2013	20:01				X		464
Indonesia	6	Aug. 12,2013	00:53				X		708
New Zealand	6.1	Aug. 12,2013	04:16				X		712
Peru	6.2	Aug. 12,2013	09:49				X		717
Colombia	6.7	Aug. 13,2013	15:43				X		9
New Sealand	6.5	Aug. 16,2013	02:31	X					68
Indian Ridge	6.1	Aug. 17,2013	16:32	X					106
Mexico	6.2	Aug. 21,2013	12:38		X				19
New Zealand	6.2	Aug. 28,2013	02:54			X			62
Alaska	7	Aug. 30,2013	16:25	X					19
Alaska	6	Aug. 31,2013	06:38	X					33
Indonesia	6.5	Sep. 01,2013	11:52	X					109
Canada	6.1	Sep. 03,2013	20:19			X			119
Izu Islands, Japan	6.5	Sep. 04,2013	00:18			X			123
Canada	6	Sep. 04,2013	00:23			X			123
Alaska M	6.5	Sep. 04,2013	02:32			X			125
Alaska	6	Sep. 04,2013	06:27			X			129
Northern Mid-Atlantic Ridge	6	Sep. 05,2013	04:01			X			151
Guatemala	6.4	Sep. 08,2013	00:13			X			219
Central East Pacific Rise	6.1	Sep. 11,2013	12:44				X		303
Alaska	6.1	Sep. 15,2013	16:21				X		392
Indonesia	6.1	Sep. 21,2013	01:39			X			61
Pakistan	7.7	Sep. 24,2013	11:29			X			143
Southern East Pacific Rise	6,1	Sep. 25,2013	06:51	X					13
Peru	7.1	Sep. 25,2013	16:42	X					23
Pakistan	6.8	Sep. 28,2013	07:34	X					85
New Zealand	6.5	Sep. 30,2013	05:55	X					130
Sea of Okhotsk	6.7	Oct.01-ott-13	03:38	X					152
Amsterdam Island	6.4	Oct.04,2013	17:26			X			240
Mariana Islands region	6	Oct.06,2013	16:38			X			287
West Chile Rise	6.2	Oct.06,2013	21:33			X			291
New Zealand	6.2	Oct.11,2013	21:25			X			84
Veneziela	6	Oct.12,2013	02:10			X			89
Greece	6.6	Oct.12,2013	13:11			X			100
Philippines	7.1	Oct.15,2013	00:12	X					28
Papua New Guinea	6.8	Oct.16,2013	10:30	X					69
Mexico	6.6	Oct.19,2013	17:54			X			141

Tonga	6	Oct.23,2013	08:23	X					66
Sandwich Islands	6.7	Oct.24,2013	19:25			X			101
Honshu, Japan	7.1	Oct.25,2013	17:10			X			123
Chile	6.2	Oct.30,2013	02:51	X					94
Taiwan	6.3	Oct.31,2013	12:02			X			128
Chile	6.6	Oct.31,2013	23:03			X			139
Easter Island region	6	Nov. 02,2013	15:52			X			179
Tonga	6.2	Nov. 02,2013	18:53			X			183
Russia	6.4	Nov. 12,2013	07:03	X					173
Scotia Sea	6.1	Nov. 13,2013	23:45			X			213
Scotia Sea	6.9	Nov. 16,2013	03:34			X			265
Scotia Sea	7.7	Nov. 17,2013	09:04			X			295
Indonesia	6	Nov. 19,2013	13:32	X					1
Mariana Islands	6	Nov. 19,2013	17:00	X					5
Fiji	6.5	Nov. 23,2013	07:48			X			91
Russia	6	Nov. 25,2013	05:56			X			137
Falkland Islands region	7	Nov. 25,2013	06:27			X			138
South Atlantic Ocean	6	Nov. 25,2013	07:21			X			139
Indonesia	6.4	Dec. 01,2013	01:24	X					29
Indonesia	6	Dec. 01,2013	06:29		X				34
Russia	6	Dec. 08,2013	17:24			X			53
Mariana Islands	6.2	Dec. 17,2013	23:38			X			134
									142 Earthquakes
Vanuatu	6.5	Jan. 01,2014	16:03			X			243
Puerto Rico	6.4	Jan. 13,2014	04:01			X			197
New Zealand	6.1	Jan. 20,2014	02:52			X			363
Tonga	6.1	Jan. 21,2014	01:29	X					9
Indonesia	6.1	Jan. 25,2014	05:14			X			110
Greece	6.1	Jan. 26,2014	13:55			X			141
Visokoi Islands	6.1	Feb. 01,2014	03:58	X					2
New Zealand	6.5	Feb. 02,2014	09:26	X					32
Greece	6	Feb. 03,2014	03:08	X					50
Vanuatu	6.5	Feb. 07,2014	08:40			X			153
Papua New Guinea	6	Feb. 09,2014	14:56			X			205
China	6.9	Feb. 12,2014	09:19	X					35
Barbados	6.5	Feb. 18,2014	09:27	X					1
Alaska	6.1	Feb. 26,2014	21:13	X					42
Nicaragua	6.3	Marc. 02,2014	09:37			X			100
Japan	6.5	Marc. 02,2014	20:11			X			111
Mexico	6	Marc. 02,2014	22:17			X			113
Vanuatu	6.3	Marc. 05,2014	09:56			X			198
California	6.8	Marc. 10,2014	05:18			X			314
Sandwich Islands	6.4	Marc. 11,2014	02:44			X			335
Papua New Guinea M6,1	6.1	Marc. 11,2014	22:03			X			355
Japan	6.3	Marc. 13,2014	17:06	X					39
Peru	6.1	Marc. 15,2014	08:59			X			78
Peru	6.3	Marc. 15,2014	23:51			X			93
Chile	6.7	Marc. 16,2014	21:16			X			115
Chile	6.4	Marc. 17,2014	05:11			X			123
India	6.4	Marc. 21,2014	13:41	X					8
Chile	6.2	Marc. 22,2014	12:59	X					30
Chile	6.2	Marc. 23,2014	18:20	X					60
Fiji	6.3	Marc. 26,2014	03:29			X			117
Solomon Islands	6	Marc. 27,2014	03:49			X			141
Chile	8.2	Apr. 01,2014	23:46			X			281
Chile	6.9	Apr. 01,2014	23:57			X			282
Panama	6	Apr. 02,2014	16:13	X					8
Chile	6.5	Apr. 03,2014	01:48	X					18
Chile	7.7	Apr. 03,2014	02:43	X					19
Chile	6.4	Apr. 03,2014	05:26	X					22
Chile	6.3	Apr. 04,2014	01:37	X					42
Solomon Islands	6	Apr. 04,2014	11:40	X					52
Nicaragua	6.1	Apr. 10,2014	23:27			X			209
Chile	6.2	Apr. 11,2014	00:01			X			210
Papua New Guinea	7.1	Apr. 11,2014	07:07			X			217
Papua New Guinea	6.5	Apr. 11,2014	08:16			X			218
Nicaragua	6.6	Apr. 11,2014	20:29			X			230
Papua New Guinea	6.1	Apr. 12,2014	05:24			X			237
Solomon Islands	7.6	Apr. 12,2014	20:14			X			252
Solomon Islands	7.4	Apr. 13,2014	12:36			X			268
Solomon Islands	6.6	Apr. 13,2014	13:24			X			269
Bouvet Island region	6.8	Apr. 15,2014	03:53			X			307

Balleny Islands region	6.2	Apr. 17,2014	15:06	X					16
Solomon Islands	6.1	Apr. 18,2014	04:13	X					27
Mexico	7.2	Apr. 18,2014	14:27	X					37
Papua New Guinea	6.6	Apr. 19,2014	01:04	X					48
Papua New Guinea	7.5	Apr. 19,2014	13:"8	X					60
Papua New Guinea	6.2	Apr. 20,2014	01:15	X					72
Canada	6.5	Apr. 24,2014	03:10			X			170
Tonga	6.1	Apr. 26,2014	06:02			X			221
New Caledonia	6.6	May 01,2014	06:36	X					4
Fiji	6.6	May 04,2014	09:15			X			78
Fiji	6.3	May 04,2014	09:25			X			78
Japan	6	May 04,2014	20:18			X			79
Thailand	6.1	May 05,2014	11:08			X			104
Chile	6.3	May 06,2014	20:52			X			137
Papua New Guinea	6	May 07,2014	04:20	X					1
Mexico	6.4	May 08,2014	17:00	X					36
Mexico	6	May 10,2014	07:36			X			76
East Pacific Rise	6.6	May 12,2014	18:35			X			135
Panama	6.5	May 13,2014	06:35			X			148
Micronesia	6.1	May 14,2014	20:46			X			185
Micronesia	6.3	May 15,2014	08:16	X					7
Philippines	6.3	May 15,2014	10:16	X					9
Sumatra	6	May 18,2014	01:02			X			72
India	6	May 21,2014	16:21	X					18
Greece	6.9	May 24,2014	09:25			X			82
Mexico	6.2	May 31,2014	11:35			X			126
South Indian Ocean	6.5	June 14,2014	11:10		X				30
Vanuatu	6.2	June 19,2014	10:17			X			23
New Zealand	6.9	June 23,2014	19:19	X					13
New Zealand	6.5	June 23,2014	19:21	X					13
New Zealand	6.7	June 23,2014	20:06	X					14
Alaska	7.9	June 23,2014	20:53	X					15
Alaska	6	June 23,2014	21:11	X					16
Alaska	6	June 23,2014	21:30	X					16
Alaska	6	June 23,2014	22:29	X					17
Alaska	6.3	June 24,2014	03:15	X					21
Japan	6.2	June 29,2014	05:56				X		144
Visokoi Island	6.9	June 29,2014	07:52				X		146
Visokoi Island	6	June 29,2014	14:32				X		153
Wallis & Fortuna	6.4	June 29,2014	15:52				X		154
Wallis & Fortuna	6.7	June 29,2014	17:15				X		156
Japan	6.2	June 30,2014	19:55				X		159
Balleny Islands	6	July 02,2014	06:53				X		241
New Zealand	6.3	July 03,2014	20:50	X					14
Papua New Guinea	6.5	July 04,2014	16:00	X					34
Indonesia	6	July 05,2014	10:39	X					52
Mexico	6.9	July 07,2014	11:23	X					101
Vanuatu	6.2	July 08,2014	12:56	X					126
Japan	6.5	July 11,2014	19:22	X					18
Philippines	6.3	July 14,2014	09:59		X				80
Alaska	6	July 15,2014	11:49			X			106
Tonga	6.2	July 19,2014	12:27			X			203
Owen Fracture Zone region	6	July 19,2014	14:14			X			205
Russia	6.2	July 20,2014	18:32			X			234
Fiji	6.9	July 21,2014	14:54				X		253
Alaska	6.1	July 25,2014	10:54				X		345
Northern Mid-Atlantic Ridge	6	July 27,2014	01:28	X					13
Northern Mid-Atlantic Ridge	6.6	July 27,2014	01:28	X					13
Mexico	6.3	July 29,2014	10:46	X					70
Papua New Guinea	6	July 29,2014	13:27	X					73
Microneria region	6.9	Aug. 03,2014	00:22			X			122
China	6.2	Aug. 03,2014	08:30			X			130
Japan	6.1	Aug. 10,2014	03:43			X			125
Iran	6.2	Aug. 18,2014	02:32		X				63
Iran	6	Aug. 18,2014	18:08			X			79
Chile	6.4	Aug. 23,2014	22:32	X					29
California	6	Aug. 24,2014	10:20	X					79
Peru	6.8	Aug. 24,2014	23:21		X				92
Tonga	6	Sept.04,2014	05:33	X					338
Easter Island region	6.1	Sept.06,2014	06:53		X				387
Mexico	6.2	Sept.06,2014	19:22			X			400
Indonesia	6.2	Sept.10,2014	02:46			X			456

Guam	6.7	Sept.17,2014	06:14			X			460
Argentina	6.2	Sept.24,2014	11:16			X			60
Solomon Islands	6.1	Sept.25,2014	09:13			X			82
Alaska	6.2	Sept.25,2014	17:51			X			90
China	6	Oct. 07,2014	13:49			X			374
Mexico	6	Oct. 08,2014	02:40			X			387
Southern East Pacific Rise	7.1	Oct. 09,2014	02:14			X			411
Southern East Pacific Rise	6.6	Oct. 09,2014	02:32			X			412
Japan	6.3	Oct. 11,2014	02:35	X					5
El Salvador	7.3	Oct. 14,2014	03:51			X			78
Kermadec Islands	6.3	Oct. 14,2014	04:12			X			79
Tonga	6.1	Oct. 25,2014	03:15			X			342
Easter Island region	6	Nov. 01,2014	10:59	X					24
Fiji	7.1	Nov. 01,2014	18:57	X					32
Papua New Guinea	6.6	Nov. 07,2014	03:33			X			160
New Caledonia	6.1	Nov. 10,2014	10:04			X			41
Inodonesia	7.1	Nov. 15,2014	02:31			X			154
New Zealand	6.7	Nov. 16,2014	22:33				X		198
Solomon Islands	6.1	Nov. 17,2014	01:06				X		201
Prince Edward Islands region	6.2	Nov. 17,2014	16:52				X		216
Indonesia	6.5	Nov. 21,2014	10:10				X		306
Japan	6.2	Nov. 22,2014	13:08				X		333
Indonesia	6.8	Nov. 26,2014	14:33	X					20
Philippines	6.3	Dec. 02,2014	05:11			X			131
Panama	6	Dec. 06,2014	17:21	X					31
Indonesia	6	Dec. 06,2014	22:05	X					35
Papua New Guinea	6.8	Dec. 07,2014	01:22		X				39
Panama	6.6	Dec. 08,2014	08:54			X			71
Taiwan	6.1	Dec. 10,2014	21:03			X			131
Indonesia	6.6	Dec. 21,2014	11:34	X					96
Philippineas	6.1	Dec. 29,2014	09:29			X			288
Fiji	6.1	Dec. 30,2014	21:17		X				15
									153 Earthquakes